

# The mass of the $\pi^-$

M. Daum<sup>1</sup> and D. Gotta<sup>2\*</sup>

<sup>1</sup> Paul Scherrer Institut, 5232 Villigen PSI, Switzerland

<sup>2</sup> Institut für Kernphysik, Forschungszentrum Jülich, 52425 Jülich, Germany

\* d.gotta@fz-juelich.de

February 22, 2021



*Review of Particle Physics at PSI*

doi:[10.21468/SciPostPhysProc.2](https://doi.org/10.21468/SciPostPhysProc.2)

## Abstract

The most precise values of the mass of the negatively charged pion have been determined from several measurements of X-ray wavelengths for transitions in pionic atoms at PSI. The Particle Data Group gives the average  $m_{\pi^-} = (139.570\ 61 \pm 0.000\ 24)$  MeV/c<sup>2</sup>.

## 10.1 Introduction

The most accurate determination of the mass of the negatively charged pion,  $m_{\pi^-}$ , is obtained from measurements of X-ray transition energies in pionic atoms. X-rays stem from a de-excitation cascade after capture into high-lying atomic states of a nucleus  $N_Z^A$  with mass number  $A$  and charge  $Z$ .

The atomic binding energies  $E_{nl}$  are directly related to the reduced mass  $\mu$  of the  $\pi N_Z^A$  system. The relativistic description of  $E_{nl}$  is given for spin 0 particles by [1]

$$E_{nl} = \frac{-\mu c^2}{2} \left( \frac{Z\alpha}{n} \right)^2 \left[ 1 + \left( \frac{Z\alpha}{n} \right)^2 \left( \frac{n}{l+1/2} - \frac{3}{4} \right) \right] + \mathcal{O}[(Z\alpha)^6]. \quad (10.1)$$

Here,  $n$  and  $l$  are the principal and angular momentum quantum numbers of the atomic level, respectively, and  $\alpha$  is the fine structure constant. The leading term of  $\mathcal{O}[(Z\alpha)^2]$  coincides with the well-known Bohr formula. (10.1) holds for  $Z \lesssim 1/(2\alpha) = 68$ .

For high-precision experiments, further contributions to  $E_{nl}$ , not included in (10.1), must be considered. Most important are QED effects, i.e. vacuum polarization, relativistic recoil ( $\mathcal{O}[(Z\alpha)^4]$ ), as well as hyperfine and strong-interaction shifts. Recent QED calculations achieve an accuracy of  $\leq \pm 1$  meV for pure electromagnetic transition energies [2].

## 10.2 Measurements at PSI

New measurements began following discussions of muon neutrino mass limits, aiming at a precision of about 1 ppm for the mass of the  $\pi^-$ . The three most recent and precise determinations of  $m_{\pi^-}$  [3] were performed at PSI, using the high pion fluxes available there. The X-ray transition energies  $E_X$  are obtained via the measurement of the angle of diffraction, the Bragg angle  $\Theta_B$ , with crystal spectrometers by using Bragg's law  $n\lambda = 2d \cdot \sin \Theta_B$ , where  $n$  is the order of reflection,  $\lambda = h/E_X$  the X-ray's wave length,  $h$  Planck's constant, and  $d$  the lattice constant of the corresponding crystal planes.

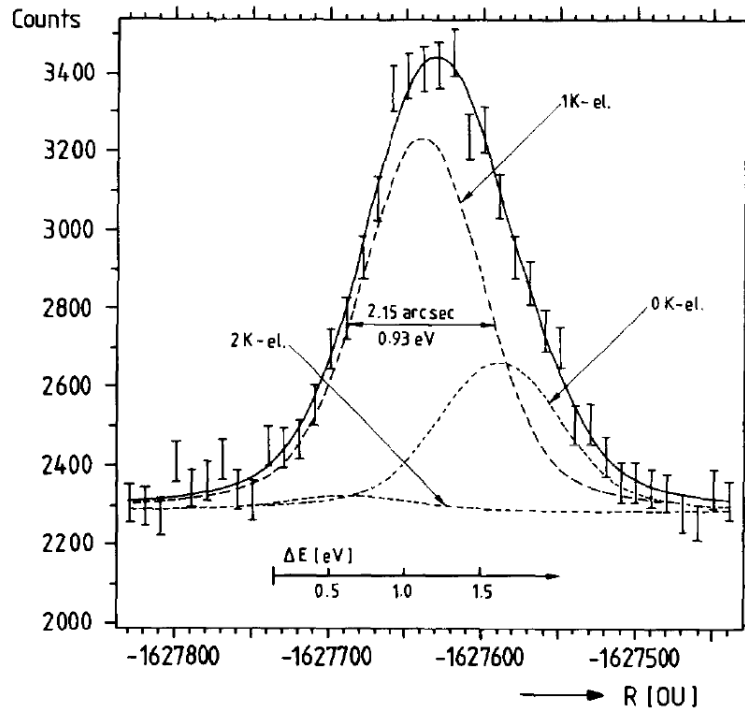


Figure 10.1: Bragg reflection of the  $(4f - 3d)$  transition in pionic  $^{24}\text{Mg}$  measured with a (110) quartz crystal in third order of diffraction; x-axis:  $R$  is the interferometer read-out in optical units (OU). The fit function is marked by the solid line; it is the sum of three individual peaks corresponding to the cases of having two, one or zero K-electrons present during the pionic transition. The line shapes of the different peaks are obtained by folding the instrumental response function with the natural line width of the transition.

30 In the first of these experiments, a DuMond crystal spectrometer was used to mea-  
 31 sure the  $\pi\text{Mg}(4f - 3d)$  transition at 26.9 keV in a solid magnesium target [4, 5]. Energy  
 32 calibration and experimental resolution were provided by the 25.7 keV  $\gamma$  line from  $^{161}\text{Tb}$   
 33 decay. The observed line width, however, was larger than the instrumental resolution of  
 34 0.93 eV (Figure 10.1). This was attributed to the occurrence of different populations of  
 35 the electronic K shell and, consequently, different screenings of the nuclear charge. Based  
 36 on a measurement of the intensity balance of the sum of the  $(nf - 3d)$  transitions to the  
 37  $(3d - 2p)$  line, which yielded a K electron shell population of  $(0.44 \pm 0.30)$ , it was origi-  
 38 nally assumed that the strongest component in the spectrum corresponds to one K-shell  
 39 electron. The corresponding result for the pion mass (solution A) is given in Table 10.1 -  
 40 entry 1986.

41 Later, this result came into strong disagreement with the continuously improved preci-  
 42 sion measurements of the muon momentum  $p_{\mu^+}$  from pion decay at rest  $\pi^+ \rightarrow \mu^+ \nu_{\mu}$  [9–11].  
 43 The lower limit thus derived for  $m_{\pi^+}$  was 3.5 standard deviations higher than the world  
 44 average for  $m_{\pi^-}$  as obtained from pionic magnesium. In addition, the squared muon  
 45 neutrino mass determined from  $p_{\mu^+}$  and  $m_{\pi^-}$  then became negative by 6 standard devia-  
 46 tions [10, 11].

47 A re-assessment of the  $\pi^-\text{Mg}(4f - 3d)$  line shape experiment led to the conclusion  
 48 that when interpreting the strongest component in Figure 10.1 as the two K-electron  
 49 contribution [6], the above-mentioned discrepancy in the  $m_{\pi^+}$  results is removed. The  
 50 alternative value for  $m_{\pi^-}$  (solution B) is given in Table 10.1 - entry 1994. This is in

| year | method  | $m_{\pi^-} / \text{MeV}/c^2$ | reference |
|------|---|------------------------------|-----------|
| 1986 | $\pi\text{Mg}(4f - 3d)/^{161}\text{Tb}\gamma$ (A) | $139.568\,71 \pm 0.000\,53$  | [4, 5]    |
| 1994 | $\pi\text{Mg}(4f - 3d)/^{161}\text{Tb}\gamma$ (B) | $139.569\,95 \pm 0.000\,37$  | [6]       |
| 1998 | $\pi\text{N}(5g - 4f)/\text{Cu}\text{K}\alpha$    | $139.570\,71 \pm 0.000\,53$  | [7]       |
| 2016 | $\pi\text{N}(5g - 4f)/\mu\text{O}(5g - 4f)$       | $139.570\,77 \pm 0.000\,18$  | [8]       |
| 2018 | $\pi^-$ PDG average                               | $139.570\,61 \pm 0.000\,23$  | [3]       |

Table 10.1: Recent results for the mass of the negatively charged pion. The PDG derived an average from the entries 1994, 1998, and 2016. The uncertainty includes a scale factor of 1.6. Earlier measurements have been omitted as they may have incorrect K-shell screening corrections [3].

51 line with the discussion on the ionization state during the de-excitation cascade, which  
 52 assumes a continuous refilling of electrons for metals [12].

53 In view of the importance of the questions involved, a new measurement of the  $\pi^-$  mass  
 54 was undertaken [7]. The increased pion flux resulting from the larger proton current in  
 55 the PSI cyclotron allowed the use of the cyclotron trap [13, 14], gas targets of about 1 bar  
 56 pressure (NTP), and a Johann-type crystal spectrometer. The big advantage of gaseous  
 57 targets is that K-electron contamination is expected to be small [12].

58 The  $(5g - 4f)$  transition in pionic nitrogen is an ideal candidate. With an energy  
 59 of 4.055 keV, the reflectivity of silicon Bragg crystals in second order and the efficiency  
 60 of X-ray detectors are close to optimum. The copper  $\text{K}\alpha_1$  fluorescence line of 8.048 keV  
 61 provides the energy calibration at practically the same Bragg angle when measured in  
 62 fourth order [7]. As in the  $\pi\text{Mg}$  case, different electron screening contributions would be  
 63 apparent as distortions of the line shape. The energy shift due to one (two) K electron(s) is  
 64  $-456$  ( $-814$ ) meV, while the spectrometer resolution is about 450 meV. The natural line  
 65 width of 8 meV is negligibly small, and strong-interaction effects in the  $4f$  level can be  
 66 estimated sufficiently accurate. The mass value derived from the  $\pi\text{N}(5g - 4f)$  transition  
 67 (Figure 10.2) is in agreement both with solution B of the  $\pi\text{Mg}$  experiment [6] and the  
 68 results deduced from  $\pi^+$ -decay [10, 11] (Table 10.1 - entry 1998).

69 In a second experiment, the two shortcomings of the Cu calibration were avoided: (i)  
 70 Spectra of fluorescence X-rays always include satellite lines from multiple ionization de-  
 71 pending on details of the excitation conditions. Therefore, measured energies may slightly  
 72 deviate from published reference values. (ii) Measuring in different orders of reflection re-  
 73 quires substantial corrections to the Bragg angle resulting in additional uncertainties [7].

74 A comparison of X-ray transition energies shows a near coincidence for  $\mu\text{O}$  and  $\pi\text{N}$ .  
 75 The muonic line provides an accurate calibration due to the precise knowledge of the muon  
 76 mass to 23 ppb [3, 15, 16]. Choosing again the  $(5g - 4f)$  lines for both atoms and using  
 77 a  $\text{O}_2/\text{N}_2$  gas mixture allows a simultaneous measurement in the same order of reflection  
 78 without any manipulation of the set-up [8] (Figure 10.3). The result of this measurement  
 79 agrees well with the previous  $\pi\text{N}$  measurement [7] (Table 10.1 - entry 2016).

80 The measured  $\pi\text{N}$  and  $\mu\text{O}$  line widths are  $\approx 800$  meV, much larger than the spectrom-  
 81 eter resolution. The increase of the widths is due to Doppler broadening from Coulomb  
 82 explosion, a recoil effect appearing in molecules [17], and, in contrast to  $\pi\text{Mg}$ , not to any  
 83 electron screening. The analysis of the  $\pi\text{N}(5g - 4f)$  line shape provides an upper limit  
 84 for the K-electron contamination of  $10^{-6}$ , which is much less than the 10% predicted by  
 85 cascade calculations [18], but corroborates the results from experiments measuring the  
 86 density dependence of X-ray yields [19]. Measuring the fine-structure splitting generated  
 87 by the angular momentum dependence in pionic atoms, gives the best available test of the

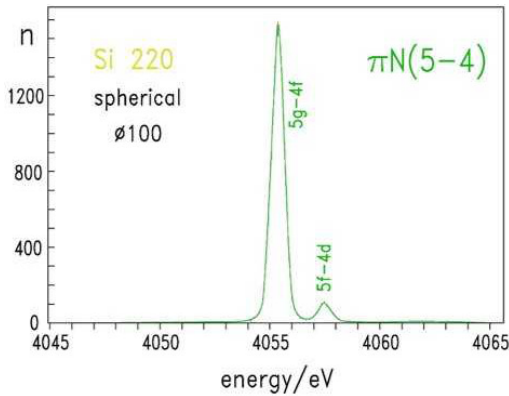


Figure 10.2:  $\pi N(5 - 4)$  complex measured with a spherically bent Si(110) crystal in  $2^{nd}$  order. The pion mass is determined from the energy of the  $\pi N(5g - 4f)$  transition (adapted from [7]).

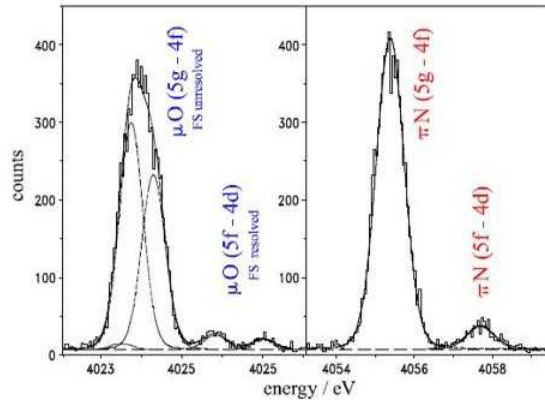


Figure 10.3:  $\pi N$  and  $\mu O(5g - 4f)$  transitions from the simultaneous measurement with an  $O_2/N_2$  (10%/90%) gas mixture at 1.4 bar pressure (adapted from [8]).

88 Klein-Gordon equation, (10.1). The recent  $\pi N(5 - 4)$  measurement (Figure 10.3) achieves  
 89 an accuracy of 0.4% for the fine-structure splitting [7], which improves earlier tests [20,21]  
 90 by one order of magnitude.

91 In conclusion, the present study demonstrates the potential of crystal spectroscopy  
 92 with bent crystals in the field of exotic atoms. As an application, X-rays of hydrogen-like  
 93 pionic atoms can be used to provide calibration standards in the few keV range, where  
 94 suitable radioactive sources are not available [22]. The accuracy of such standards is given  
 95 by the present uncertainty of the pion mass [2].

96 Facing the fact that pion beams at PSI provide a flux of about  $10^9/s$ , the use of  
 97 double-flat crystal spectrometers may be considered allowing for absolute angle calibra-  
 98 tions choosing specific narrow hydrogen-like pionic transitions not affected by Coulomb  
 99 explosion, e. g. from pionic neon. A precision for the pion mass determination of the order  
 100 of 0.5 ppm would be feasible. A method based on laser spectroscopy of metastable pionic  
 101 helium, if successfully applied, could further improve significantly on the accuracy for the  
 102  $\pi^-$  mass [23–25].

## 103 References

- 104 [1] T. Ericson and W. Weise, *Pions and Nuclei*, Clarendon Press, New York (1988).  
 105 [2] M. Trassinelli and P. Indelicato, *Relativistic calculations of pionic and*  
 106 *kaonic atoms hyperfine structure*, Phys. Rev. **A76**, 012510 (2007),  
 107 doi:10.1103/PhysRevA.76.012510, physics/0611263.  
 108 [3] M. Tanabashi *et al.*, *Review of particle physics*, Phys. Rev. D **98**, 030001 (2018),  
 109 doi:10.1103/PhysRevD.98.030001.  
 110 [4] B. Jeckelmann *et al.*, *New Precision Determination of the  $\pi^-$  Mass From Pionic*  
 111 *X-rays*, Phys. Rev. Lett. **56**, 1444 (1986), doi:10.1103/PhysRevLett.56.1444.  
 112 [5] B. Jeckelmann *et al.*, *New Precision Determination of the  $\pi^-$  Mass From Pionic*  
 113 *X-rays*, Nucl. Phys. **A457**, 709 (1986), doi:10.1016/0375-9474(86)90476-8.

- 114 [6] B. Jeckelmann, P. F. A. Goudsmit and H. J. Leisi, *The Mass of the negative pion*,  
115 Phys. Lett. **B335**, 326 (1994), doi:[10.1016/0370-2693\(94\)90358-1](https://doi.org/10.1016/0370-2693(94)90358-1).
- 116 [7] S. Lenz *et al.*, *A New determination of the mass of the charged pion*, Phys. Lett.  
117 **B416**, 50 (1998), doi:[10.1016/S0370-2693\(97\)01337-3](https://doi.org/10.1016/S0370-2693(97)01337-3).
- 118 [8] M. Trassinelli *et al.*, *Measurement of the charged pion mass using X-ray spectroscopy*  
119 *of exotic atoms*, Phys. Lett. **B759**, 583 (2016), doi:[10.1016/j.physletb.2016.06.025](https://doi.org/10.1016/j.physletb.2016.06.025),  
120 [1605.03300](https://doi.org/10.1016/j.physletb.2016.06.025).
- 121 [9] M. Daum, R. Frosch, D. Herter, M. Janousch and P. R. Kettle, *New precision mea-*  
122 *surement of the muon momentum in pion decay at rest*, Phys. Lett. **B265**, 425 (1991),  
123 doi:[10.1016/0370-2693\(91\)90078-5](https://doi.org/10.1016/0370-2693(91)90078-5).
- 124 [10] K. Assamagan *et al.*, *Measurement of the muon momentum in pion decay at rest using*  
125 *a surface muon beam*, Phys. Lett. **B335**, 231 (1994), doi:[10.1016/0370-2693\(94\)91419-](https://doi.org/10.1016/0370-2693(94)91419-2)  
126 [2](https://doi.org/10.1016/0370-2693(94)91419-2).
- 127 [11] K. Assamagan *et al.*, *Upper limit of the muon-neutrino mass and charged pion mass*  
128 *from momentum analysis of a surface muon beam*, Phys. Rev. **D53**, 6065 (1996),  
129 doi:[10.1103/PhysRevD.53.6065](https://doi.org/10.1103/PhysRevD.53.6065).
- 130 [12] R. Bacher, D. Gotta, L. M. Simons, J. H. Missimer and N. C. Mukhopadhyay, *On*  
131 *Muonic Atoms With Vacant Electron Shells*, Phys. Rev. Lett. **54**, 2087 (1985),  
132 doi:[10.1103/PhysRevLett.54.2087](https://doi.org/10.1103/PhysRevLett.54.2087).
- 133 [13] L. M. Simons, *Recent results on anti-protonic atoms using a cyclotron trap at lear*,  
134 Phys. Scripta **T22**, 90 (1988), doi:[10.1088/0031-8949/1988/T22/013](https://doi.org/10.1088/0031-8949/1988/T22/013).
- 135 [14] L. M. Simons, *The cyclotron trap for antiprotons*, Hyperfine Interact. **81**, 253 (1993),  
136 doi:[10.1007/BF00567270](https://doi.org/10.1007/BF00567270).
- 137 [15] W. Liu *et al.*, *High precision measurements of the ground state hyperfine structure*  
138 *interval of muonium and of the muon magnetic moment*, Phys. Rev. Lett. **82**, 711  
139 (1999), doi:[10.1103/PhysRevLett.82.711](https://doi.org/10.1103/PhysRevLett.82.711).
- 140 [16] P. J. Mohr, D. B. Newell and B. N. Taylor, *CODATA Recommended Values of*  
141 *the Fundamental Physical Constants: 2014*, Rev. Mod. Phys. **88**(3), 035009 (2016),  
142 doi:[10.1103/RevModPhys.88.035009](https://doi.org/10.1103/RevModPhys.88.035009), [1507.07956](https://arxiv.org/abs/1507.07956).
- 143 [17] T. Siems, D. F. Anagnostopoulos, G. Borchert, D. Gotta, P. Hauser, K. Kirch, L. M.  
144 Simons, P. El-Khoury, P. Indelicato, M. Augsburg, D. Chatellard and J.-P. Egger,  
145 *First direct observation of coulomb explosion during the formation of exotic atoms*,  
146 Phys. Rev. Lett. **84**, 4573 (2000), doi:[10.1103/PhysRevLett.84.4573](https://doi.org/10.1103/PhysRevLett.84.4573).
- 147 [18] V. R. Akylas and P. Vogel, *Muonic Atom Cascade Program*, Comput. Phys. Commun.  
148 **15**, 291 (1978), doi:[10.1016/0010-4655\(78\)90099-1](https://doi.org/10.1016/0010-4655(78)90099-1).
- 149 [19] K. Kirch, D. Abbott, B. Bach, P. Hauser, P. Indelicato, F. Kottmann, J. Missimer,  
150 P. Patte, R. T. Siegel, L. M. Simons and D. Viel, *Muonic cascades in isolated low-z*  
151 *atoms and molecules*, Phys. Rev. A **59**, 3375 (1999), doi:[10.1103/PhysRevA.59.3375](https://doi.org/10.1103/PhysRevA.59.3375).
- 152 [20] K. C. Wang, F. Boehm, A. A. Hahn, H. E. Henrikson, J. P. Miller, R. J. Powers,  
153 P. Vogel, J. L. Vuilleumier and R. Kunselman, *Experimental Determination of the*  
154 *Relativistic Fine Structure Splitting in a Pionic Atom*, Phys. Lett. **79B**, 170 (1978),  
155 doi:[10.1016/0370-2693\(78\)90461-6](https://doi.org/10.1016/0370-2693(78)90461-6).

- 156 [21] L. Delker, G. Dugan, C. S. Wu, D. C. Lu, A. J. Caffrey, Y. T. Cheng and  
157 Y. K. Lee, *Experimental verification of the relativistic fine-structure term of the*  
158 *klein-gordon equation in pionic titanium atoms*, Phys. Rev. Lett. **42**, 89 (1979),  
159 doi:[10.1103/PhysRevLett.42.89](https://doi.org/10.1103/PhysRevLett.42.89).
- 160 [22] D. F. Anagnostopoulos, D. Gotta, P. Indelicato and L. M. Simons, *Low-Energy X-*  
161 *Ray Standards from Hydrogenlike Pionic Atoms*, Phys. Rev. Lett. **91**, 240801 (2003),  
162 doi:[10.1103/PhysRevLett.91.240801](https://doi.org/10.1103/PhysRevLett.91.240801).
- 163 [23] M. Hori, V. I. Korobov and A. Sótér, *Proposed method for laser spectroscopy of pionic*  
164 *helium atoms to determine the charged-pion mass*, Phys. Rev. **A 89**, 042515 (2014),  
165 doi:[10.1103/PhysRevA.89.042515](https://doi.org/10.1103/PhysRevA.89.042515).
- 166 [24] M. Hori, H. Aghai-Khozani, A. Sótér, A. Dax and D. Barna, *Laser spectroscopy of*  
167 *pionic helium atoms*, Nature **581**, 37 (2020), doi:[10.1038/s41586-020-2240-x](https://doi.org/10.1038/s41586-020-2240-x).
- 168 [25] M. Hori, H. Aghai-Khozani, A. Sótér, A. Dax and D. Barna, *Recent results of laser*  
169 *spectroscopy experiments of pionic helium atoms at PSI*, SciPost Phys. Proc. **2**, ppp  
170 (2021), doi:[10.21468/SciPostPhysProc.2.XXX](https://doi.org/10.21468/SciPostPhysProc.2.XXX).